

Tidal instability in a rotating and differentially heated ellipsoidal shell

D. Cébron^{*}, P. Maubert, M. Le Bars

*Institut de Recherche sur les Phénomènes Hors Equilibre, UMR 6594,
CNRS et Aix-Marseille Université, 49 rue F. Joliot-Curie, BP146, 13384 Marseille Cedex 13, France.*

Received 2010 February 23; in original form 2010 February 23

SUMMARY

The stability of a rotating flow in a triaxial ellipsoidal shell with an imposed temperature difference between inner and outer boundaries is studied numerically. We demonstrate that (i) a stable temperature field encourages the tidal instability, (ii) the tidal instability can grow on a convective flow, which confirms its relevance to geo- and astrophysical contexts, and (iii) its growth rate decreases when the intensity of convection increases. Simple scaling laws characterizing the evolution of the heat flux based on a competition between viscous and thermal boundary layers are derived analytically and verified numerically. Our results confirm that thermal and tidal effects have to be simultaneously taken into account when studying geophysical and astrophysical flows.

Key words: tides, tidal/elliptical instability, planetary cores, finite element numerical simulations, convection, stratification, Nusselt number.

1 INTRODUCTION

The tidal or elliptical instability comes from a triadic parametric resonance between two inertial waves of a rotating fluid and an imposed elliptic deformation (see for instance the review by Kerswell 2002, and references therein). It is a generic phenomenon in turbulence (e.g. Widnall et al. 1974; Moore and Saffman 1975) and vortex dynamics (e.g. Leweke and Williamson 1998; Le Dizès and Laporte 2002; Meunier et al. 2002). There, the elliptical deformation comes from interactions between adjacent vortices. But this instability is also studied in geophysical and astrophysical tidally deformed bodies: for example, its presence has been suggested (i) in binary stars (Rieutord 2003; Le Bars et al. 2010) and accretion disks (Goodman 1993; Ryu and Goodman 1994), where they could participate in the energy and angular momentum exchanges between neighbouring systems (Lubow et al. 1993), and (ii) in planetary cores (e.g. Aldridge et al. 1997; Cébron et al. 2010), where they could play an important role in the induction of a magnetic field (Kerswell and Malkus 1998; Lacaze et al. 2006; Herreman et al. 2009) and even in planetary dynamos (Malkus 1993).

Previous studies of tidal instability have been performed for an isothermal fluid, starting from a solid body rotation or from an homogeneous isotropic turbulent rotating flow (Fabijonas and Holm 2003). Nevertheless, in all natural systems, temperature differences are also present, which lead either to stratification or to convection. The previous studies need then to be reinvestigated in order to quantify the impact of a temperature field on the elliptical instability. Conversely, from a thermal point of view, many studies have been performed regarding the convective flow of an incompressible homogeneous fluid in a rotating spherical shell (see for instance Aurnou 2007, and references therein). However, since most astrophysical bodies are tidally deformed, these studies have to be reinvestigated to account for the potential presence of an elliptical instability. Note that a link between tidal resonance of gravito-inertial waves and thermal effects has been proposed by Kumazawa et al. (2006) in a geophysical context. However, this study considers the resonant forcing of a given wave by tides, which is different from the elliptical instability possibly induced by parametric resonance. Then, to the best of our knowledge, the only previous work which combines thermal and elliptical effects is the theoretical study of Le Bars and Le Dizès (2006), who considered the influence of an established diffusive temperature profile. They then interpreted the thermo-elliptical instability in terms of gravito-inertial waves resonance and determined its linear growth rate by a local approach. In order to complete this work,

^{*} corresponding author (cebron@irphe.univ-mrs.fr)

a guideline of our study is given by the following questions: (i) how is the growth rate of the tidal instability modified by an imposed temperature difference in the spheroidal geometry? (ii) Does the tidal instability grow over an established convective flow? (iii) Is the heat flux modified by the instability, and what are the scaling laws involved? In this paper, we tackle these questions using a systematic numerical study of the thermo-elliptical rotating flow in a fixed triaxial ellipsoidal shell. The numerical model is presented in section 2. The variations of the heat flux and the growth rate are systematically quantified and interpreted in section 3. Finally, orders of magnitude and conclusions are drawn for geo- and astrophysical flows in section 4.

2 NUMERICAL MODEL AND ITS VALIDATION

As sketched in figure 1, we consider the rotating flow inside a fixed triaxial ellipsoid of axes (a, b, c) , with a constant tangential velocity $U\sqrt{1 - (z/c)^2}$ imposed all along the outer boundary in each plane of coordinate z perpendicular to the rotation axis (Oz) , where U is the imposed boundary velocity at the equator. An homothetic ellipsoidal core, in a ratio $\eta = 0.3$, is placed at the center, with also an imposed constant tangential velocity $\eta U\sqrt{1 - (z/c)^2}$ along its boundary. In the following, we use the mean equatorial radius $R_{eq} = (a + b)/2$ as a lengthscale and we introduce the timescale Ω^{-1} by writing the tangential velocity along the deformed outer boundary at the equator $U = \Omega R_{eq}$. Then, the problem is fully described by the adimensionalized Navier-Stokes equations with four dimensionless numbers: the eccentricity $\varepsilon = (b^2 - a^2)/(a^2 + b^2)$, the inner to outer core ratio η , the aspect ratio c/b , and the Reynolds number $Re = \Omega R_{eq}^2/\nu$, or its inverse the Ekman number E_k , where ν is the kinematic viscosity of the fluid. In all the computations presented here, we choose c equal to the mean equatorial radius $R_{eq} = (a + b)/2$, as in classical experimental setups (see e.g. Lacaze et al. (2005)). This allows us to focus on the well-known stationary spin-over mode of the tidal instability. Note that for lots of tidally deformed planetary and stellar bodies, the c -axis is the shortest axis because of the rotational flattening, whereas the longest axis is the one pointing towards the tide-raising body. In this configuration, the first selected mode of the tidal instability close to threshold may change (Kerswell and Malkus (1998), Cébron et al. (2010)), giving rise to oscillatory motions. Nevertheless, we expect the main physical processes described here to remain valid for these other modes.

In addition to these purely hydrodynamic considerations, we also solve the temperature equation with constant and uniform temperatures T_i and T_e applied respectively at the inner and outer boundaries. To model the buoyancy, the density is assumed to vary linearly with the temperature and the Boussinesq approximation is used. Then, the gravity term of the Navier-Stokes equation is written: $\rho \mathbf{g}_* = \rho(T_e) [1 - \alpha(T_* - T_e)] \mathbf{g}_*$, where ρ is the fluid density, α the coefficient of thermal volumic expansion, \mathbf{g}_* the local gravity which depends on the position and T_* the local temperature. In our model, the gravity is calculated by solving the Poisson equation for the gravitational potential ϕ , assuming that the outer boundary is an isopotential. Thus, the thermal part of the problem is controlled by two dimensionless numbers: the Prandtl number $Pr = \nu/\kappa$, where κ is the thermal diffusivity, and the Rayleigh number $Ra = (\alpha g_0 (T_i - T_e) d^3)/(\kappa \nu)$, where $d = R_{eq}(1 - \eta)$ is the shell thickness and g_0 is the surface gravity at the outer boundary of the corresponding sphere, i.e. $g_0 = 4/3 \pi G R_{eq} \rho(T_e)$ with G the gravitational constant. Note that the kinematic viscosity of the fluid is assumed independent of the temperature in this work.

Finally, the problem solved is described by the following system of dimensionless equations:

$$\frac{\partial \mathbf{u}}{\partial t} + \mathbf{u} \cdot \nabla \mathbf{u} = -\nabla p + \frac{1}{Re} \Delta \mathbf{u} - \frac{Ra}{Pr Re^2 (1 - \eta)^3} T \mathbf{g}, \quad (1)$$

$$\nabla \cdot \mathbf{u} = 0, \quad (2)$$

$$\frac{\partial T}{\partial t} + \mathbf{u} \cdot \nabla T = \frac{1}{Pr Re} \Delta T, \quad (3)$$

$$\Delta \phi = 3, \quad (4)$$

$$\mathbf{g} = -\nabla \phi, \quad (5)$$

where T is the dimensionless temperature anomaly $T = (T_* - T_e)/(T_i - T_e)$. All boundary conditions have been described above. This numerical setup is a simple model for a tidally deformed liquid planetary core with a solid inner core and an imposed temperature contrast. Note that in a geophysical context, because of the compressibility, the temperature difference $\Delta T = T_i - T_e$ to consider is the superadiabatic temperature difference between the inner core boundary and the core-mantle boundary (CMB). All dimensionless numbers as well as explored numerical ranges and typical values for the Earth's and Io's cores are given in table 1.

Since there is no simple symmetry in the studied configuration, the fast and precise spectral methods classically used in planetary cores studies are not relevant here. Our computations are performed with a commercial software using a finite

element method, which allows to correctly reproduce the geometry and to simply impose the boundary conditions. An unstructured mesh with tetrahedral elements was created. The mesh element type employed is the standard Lagrange element $P1 - P2$, which is linear for the pressure field but quadratic for the velocity field. The temporal solver is IDA (Hindmarsh et al. 2005), based on backward differencing formulas. At each time step the system is solved with the sparse direct linear solver PARDISO[†].

The numerical procedure is the same for all the computations presented in this paper: starting from a fluid at rest in a spherical shell of radius R_{eq} with a diffusive temperature profile, the shell is set in rotation at a constant angular velocity Ω and a first statistically stationary state is obtained by solving the Navier-Stokes and temperature equations; then, the spherical shell is instantaneously deformed to the chosen triaxial ellipsoidal shape and we follow the dynamics. Note that this instantaneous deformation allows to study the growth rate of the elliptical instability on a well-known conductive or convective base flow. But we have also performed computations with a gradual increase of the deformation, as well as computations starting from a deformed shell with a fluid at rest before imposing the rotation at the boundaries: the classical isothermal tidal instability then grows, which is only slightly modified by then imposing a temperature difference. In all cases, the final steady-state is the same.

Two quantities are systematically studied: (i) the growth rate σ of the tidal instability, which quantifies the feedback of the temperature field on the elliptical instability, and (ii) the Nusselt number Nu , which quantifies the feedback of the elliptical instability on the thermal properties of the system. Since the elliptical instability induces a strong three-dimensional destabilization of the initial flow, the growth rate σ is determined as the time constant of the exponential growth of the mean value of the vertical velocity $W = \frac{1}{V} \int_V |w| d\tau$, where w stands for the dimensionless vertical velocity and V for the volume of the ellipsoidal shell. The Nusselt number is calculated by dividing the measured mean heat flux at the outer boundary (once a statistically stationary state is reached) by the theoretical value of the conductive heat flux in a sphere of radius R_{eq} . It has systematically been checked that the difference between this analytically known flux and the numerically calculated flux for a purely conductive ellipsoid is below 2% for our all simulations.

The purely hydrodynamic part of the numerical simulation has already been validated in Cébron et al. (2010). A complementary validation of the resolution of thermal effects has been done by computing the heat flux in a rotating spherical shell: in figure 2 (a), our results at $Re = 344$ are compared with the compilation of results given in Aurnou (2007) for the modified Nusselt number defined by $Nu^* = \frac{Nu E}{Pr}$, where $E = \frac{\nu}{\Omega d^2}$ is the Ekman number based on the gap width, i.e. $E = ((1 - \eta)^2 Re)^{-1}$. Note that our numerical results fill an area with few data and agree with the general trend. Besides, our results are compared in figure 2 (b) with the scaling law proposed by Christensen (2002) obtained from numerical simulations:

$$Nu^* = 0.077 (Ra_Q^*)^{5/9} \tag{6}$$

where $Ra_Q^* = Ra Nu E^3 / Pr^2$ is the Rayleigh number based on the heat flux instead of the temperature contrast and which does not take into account any viscous or thermal diffusive effect. An excellent quantitative agreement is found.

3 INTERACTION BETWEEN THE ELLIPTICAL INSTABILITY AND THE THERMAL FIELD

In their analytical WKB analysis of the linear stability of elliptical streamlines in the presence of a diffusive temperature field, Le Bars and Le Dizès (2006) found an analytical expression of the inviscid growth rate of the elliptical instability in the limit of small deformations as:

$$\sigma = \frac{9 - 3\tilde{Ra}}{16 - 4\tilde{Ra}} \varepsilon, \tag{7}$$

where $\tilde{Ra} = \frac{\eta - 1}{\ln(\eta)} \frac{Ra E^2}{Pr}$ is a modified Rayleigh number. The expression 7 reflects the modification by thermal effects of the elliptical instability, which in this context corresponds to the parametric resonance of 2 gravito-inertial waves with the tidal deformation. Le Bars and Le Dizès (2006) also showed that the elliptical instability cannot grow for $\tilde{Ra} > 3$ because no resonance between inertial modes is then possible. As shown in figure 3 (a), the same decreasing trend with Ra is recovered in the spherical shell, even if the results differ quantitatively from this theoretical local estimate. The first noticeable result from our complete calculations is that the growth rate of the elliptical instability is significantly enhanced by the thermal stratification (i.e. $Ra < 0$), as first suggested by Le Bars and Le Dizès (2006). It may seem at first surprising that an a priori stabilizing effect leads to an encouragement of flow destabilization, but such a behavior has already been shown for instance in a Taylor-Couette flow, where a stable configuration can be destabilized by the presence of an axial stratification, leading to the so-called strato-rotational instability (see for instance the recent experiments by Le Bars and Le Gal 2007). The second result of planetary relevance is that the tidal instability can still grow on an established convective flow. As shown in figure 4, the organization of the flow is then completely changed. Indeed, in the absence of tidal instability, the convective flow organizes

[†] www.pardiso-project.org

in a classical columnar structure shown in figure 4 (a) (the so-called Busse columns), where motions are mainly bidimensional and vertical velocities remain small, coming only from the Ekman pumping inside the columns. On the contrary in figure 4 (b), Busse columns are completely destroyed by the tidal instability, whose velocity field is fully three-dimensional. The growth rate σ of the elliptical instability progressively decreases when the Rayleigh number increases as shown in figure 3 (a). Indeed, the thermal convective motions can be seen as a perturbation superimposed on the classical isothermal base flow of the elliptical instability, corresponding to a rotation along elliptical streamlines: when the Rayleigh number increases, the typical convective velocity increases and the ellipticity of the base flow streamlines is less and less felt by the fluid particles. The dimensionless version of this model can be quantified in defining the typical Rossby number of the flow, i.e. the ratio between the root mean square convective velocity and the typical rotating velocity ΩRe_q : $Ro = \sqrt{\frac{1}{V} \int \mathbf{u} \cdot \mathbf{u} \, d\tau}$, where \mathbf{u} is the dimensionless velocity in the rotating frame. One would expect to find a critical Rossby number of order 1 for the disappearance of the tidal instability. As shown in figure 3 (b), the critical value $Ro \approx 0.25$, where the growth rate is zero, is indeed found for $Pr = 1$ and $Re = 344$, which is near the threshold of the tidal instability. The critical Rossby number then seems to increase with the Reynolds number (see figure 3 (a) for $Re = 688$), if it exists at all. Indeed, when the Rayleigh number increases, the typical convective velocity also increases whereas the typical lengthscale of convection L_{conv} simultaneously decreases. In the limit of very large Rayleigh numbers, L_{conv} is very small and turbulent motions become fully tridimensional. We then expect thermal convective motions to be seen as an effective turbulent viscosity, where the results of Fabijonas and Holm (2003) predict an encouragement of the tidal destabilization. The extensive study of this regime is very interesting, but currently out of reach of our numerical resources. Nevertheless, our current results allow to use the critical Rossby number $Ro_c = 0.25$ determined previously for $Re = 344$ as a lower bound for flow at larger Reynolds numbers. This result is sufficient for the planetary applications that we are interested in, as will be shown in the next section.

When thermal and tidal instabilities are simultaneously present, heat transfers are determined by the competition between the natural thermal convection and the forced convection due to the elliptical instability. In the latter case, the flow driven by the instability can be schematically described by three distinct regions: a fully mixed and isothermal bulk, and viscous boundary layers at the outer and inner boundaries, where the temperature is purely diffusive. The advective heat flux driven by the tidal instability is then determined by the size of the viscous boundary layers δ_ν , following $Nu - 1 \sim d/\delta_\nu$. With the classical scaling law of viscous boundary layers, we obtain $Nu - 1 = \alpha_1/\sqrt{E^*}$, where α_1 is a constant, $E^* = \frac{\nu}{u_{ei} d}$ the Ekman number associated with the flow driven by the instability, and u_{ei} the fluid velocity due to the elliptical instability. As shown in Cébron et al. (2010), this velocity u_{ei} may be computed numerically in the absence of temperature gradient by subtracting to the computed flow the theoretical base flow corresponding to an imposed rotation along elliptical streamlines. $\frac{u_{ei}}{\Omega Re_q}$ generally scales as $\alpha_2 \sqrt{Re - Re_c}$ near the threshold of instability, where $\alpha_2 \approx 0.036$ has been determined numerically and where Re_c is the critical Reynolds number for the onset of tidal instability equal to $Re_c = (5.24/\varepsilon)^2$ in the isothermal case for a stationary deformation. $\frac{u_{ei}}{\Omega Re_q}$ then saturates toward 1 far from the threshold. Keeping the same scaling in the presence of thermal effects, we expect the Nusselt number to vary as:

$$Nu - 1 = \alpha_1 \sqrt{\alpha_2 (1 - \eta)} \left(\frac{Re}{Re_c} - 1 \right)^{1/4} \sqrt{Re}. \quad (8)$$

Our numerical results shown in figure 5 (a) validate this scaling with $\alpha_1 \approx 0.01$. Far from threshold, $E^* = E$ and the scaling law becomes

$$Nu = \alpha_1 / \sqrt{E}. \quad (9)$$

Note that according to this model, the Nusselt number is a measure of the amplitude of the instability. Then, the agreement between our results and the scaling law confirms that the amplitude of the instability is not inhibited by a strong stratification, provided that the Reynolds number is far enough from the threshold.

The systematic evolution of the Nusselt number with the Rayleigh number is shown in figure 5 (b). In the absence of tidal and convective instabilities, Nu remains equal to 1. In the presence of tidal instability, the heat flux remains constant at a value larger than 1 up to a transition Rayleigh number which depends on Re , where the natural convection becomes more efficient than the forced one. Indeed, (8) and (9) describe the heat flux by the forced convection only, and are valid in particular for stably-stratified regimes and before the onset of convection $Ra < Ra_c$. But following King et al. (2009), once $Ra > Ra_c$ and convective and tidal instabilities are competing, the heat transfer is determined by the most efficient mechanism. Following scaling laws (6) and (9), the transition between the forced convection and the natural convection appears for the transition Nusselt number $Nu_t^* = \frac{Nu E}{Pr} = 0.077 (Ra_Q^*)^{5/9} = \alpha_1 \frac{\sqrt{E}}{Pr}$, which corresponds to the transition Rayleigh number:

$$Ra_t \approx 2.5 E^{-8/5} Pr^{1/5}. \quad (10)$$

For $Ra > Ra_t$, heat transfers are controlled by the natural convective motions, whereas for $Ra < Ra_t$, heat transfers are controlled by the tidal instability. For planetary applications, it is more convenient to write this result in term of flux Rayleigh number defined by $Ra_f = Ra Nu$, for which the transition appears at

$$Ra_{f,t} \approx 0.025 E^{-21/10} Pr^{1/5}. \quad (11)$$

4 PLANETARY AND STELLAR APPLICATIONS

As explained in details by Sumita and Yoshida (2002), a stable density stratification may have existed in the whole early Earth outer core and could even have been sufficiently large to prevent dynamo action. This initial stratification has been disrupted by some mechanism, which could have been either a gradual mechanism, including encroachment and entrainment (Lister and Buffett 1998), or catastrophic mechanisms driven for instance by the 1/3-annual forced nutation (Williams 1994) or by tidal resonant forcing of inertial-gravity waves (Kumazawa et al. 2006). Our work suggests an alternative proposal based on a parametric triadic resonance of gravito-inertial waves. Note that since the stratification enhances the growth rate of the tidal instability and since the early Earth was already unstable from a purely hydrodynamic analysis (Cébron et al. 2010), then a fortiori with a thermal stratification, the tidal instability can be a mechanism for this overturn, hence playing a role in one of the major events in geological Earth history.

We can also apply the heat transfer scaling laws obtained in the previous section to the present convective state of the Earth's core. Following Christensen and Aubert (2006), the typical values are $E \approx 5 \cdot 10^{-15}$, $Ra_Q^* \approx 3 \cdot 10^{-13}$ and $Ra_f \approx 10^{29}$ for $Pr = 0.25$. The first consequence that we can deduce is that $Ro \sim 10^{-6}$ according to the scaling law $Ro = 0.85 (Ra_Q^*)^{0.41}$ given by Christensen and Aubert (2006), which is significantly below the lower bound for disappearance of elliptical instability $Ro_c \approx 0.25$ found in section 3. That means that the convection does not prevent the development of the tidal instability. Besides, the scaling law (11) gives the estimate $Ra_{f_t} \sim 2 \times 10^{28}$. The Earth's core is just above the transition between the two kind of convections considered in section 3 and its heat flux is thus controlled by natural convection. However, the closeness of the values obtained here does not preclude a tidally dominated flux in previous times or in other planetary systems, and in any case highlights the relevance of the elliptical instability as one of the major process at work in planetary cores.

To finish with, many authors have assumed that the top of the Earth core is stably stratified, this layer being the so-called ocean of the core (see for instance Stanley and Mohammadi (2008) for a recent review of the literature on this subject). Actually, as described in this recent work, many clues lead to the idea that several planets contain stably stratified layers in their electrically conducting regions. An opposite (but dynamically similar) situation occurs in stars under the photosphere, where the stratified radiative zone takes place under the so-called convective zone. Then, we can address the simple following questions: in such a bi-layer flow, can the elliptical instability grow? In which area, i.e. the stratified zone, the convective zone or both? And is the heat flux completely modified by the instability? A single simulation is presented in figure 6 as an illustration of the answer. In this simulation, the same temperature $T = 0$ is imposed at boundaries, and a temperature $T = 1$ is imposed at an internal neutral boundary corresponding to an homothetic ellipsoid in a ratio $\eta_2 = 0.7$: this allows to obtain a stratified inner layer and a convective outer layer, with clearly visible convective cells (figure 6 (a)). Once the tidal instability is excited, figure 6 (b) shows that the instability grows over the whole fluid and controls the heat flux. Hence in presence of the elliptical instability, a thermal stratification (i.e. a subadiabatic temperature profile) is not synonymous of thermal isolation, which is a key point from a geophysical point of view.

5 CONCLUSION

This paper presents the first numerical study of the interaction between the tidal instability and a thermal field. Even if the range of parameters (e.g. the Reynolds number) accessible to our numerical tool is relatively limited, we have validated general physical processes of direct relevance for planetary dynamics. We have shown that a stable temperature field encourages the tidal instability. We have demonstrated also that the tidal instability can grow on a convective flow, and may disrupt the famous Busse columns in planetary cores. Finally, we have demonstrated that the heat flux at planetary scales may be controlled by the forced convection due to this tidal instability, which in any case plays a fundamental role in the organization of fluid motions.

REFERENCES

- Aldridge, K., Seyed-Mahmoud, B., Henderson, G., van Wijngaarden, W., 1997. Elliptical instability of the Earth's fluid core. *Phys. Earth Planet. Int.* 103, 365–74.
- Aurnou, J. M., 2007. Planetary core dynamics and convective heat transfer scaling. *Geophysical and Astrophysical Fluid Dynamics*, Volume 101, Numbers 5-6, pp. 327-345(19).
- Cébron, D., Le Bars, M., Leontini, J., Maubert, P., Le Gal, P., 2010. A systematic numerical study of the tidal instability in a rotating ellipsoid. Submitted to *Phys. Earth Planet. Int.*
- Christensen, U. R., 2002. Zonal flow driven by strongly supercritical convection in rotating spherical shells. 470:115-133.
- Christensen, U. R., Aubert, J., 2006. Scaling properties of convection-driven dynamos in rotating spherical shells and application to planetary magnetic fields. *Geophysical Journal International*, vol. 166 Issue 1, pp. 97 - 114.
- Fabijonas, B. R., Holm, D. D., 2003. Mean effects of turbulence on elliptic instability in fluids. *Phys. Rev. Lett.* 90, 124501.
- Gledzer, E. B., Ponomarev, V. M., 1977. Finite dimensional approximation of the motions of incompressible fluid in an ellipsoidal cavity. *Izv. Atmos. Ocean. Phys.* 13, 565–569.

- Gledzer, E. B., Dolzhansky, F. V., Obukhov, A. M., Ponomarev, V. M., 1975. An experimental and theoretical study of the stability of motion of a liquid in an elliptical cylinder. *Izv. Atmos. Ocean. Phys.* 11, 617–622.
- Goodman, J., 1993. A local instability of tidally distorted accretion disks. *Ap. J.* 406:596-613.
- Herreman, W., Le Bars, M., Le Gal, P., 2009. On the effects of an imposed magnetic field on the elliptical instability in rotating spheroids. *Phys. Fluids* 21, 046602.
- Hindmarsh, A. C., Brown, P. N., Grant, K. E., Lee, S. L., Serban, R., Shumaker, D. E., Woodward, C. S., 2005. Suite of Nonlinear and Differential/Algebraic Equation Solvers. *ACM T. Math. Software*, vol. 31, p. 363.
- Kerswell, R. R., 2002. Elliptical instability. *Annual Review of Fluid Mechanics* 34, 83–113.
- Kerswell, R. R., 1994. Tidal excitation of hydromagnetic waves and their damping in the Earth. *J. Fluid Mech.* 274, 219–241.
- Kerswell, R. R., Malkus, W. V. R., 1998. Tidal instability as the source for Io’s magnetic signature. *Geophys. Res. Lett.* 25, 603–6.
- King, E. M., Stellmach, S., Noir, J., Hansen, U., Aurnou, J. M., 2009. Boundary layer control of rotating convection systems. *Nature* 457, 301-304.
- Kumazawa, M., Yoshida, S., Ito, T., Yoshioka, H., 1994. Archaean-Proterozoic boundary interpreted as a catastrophic collapse of the stable density. *Jour. Gel. Soc. Japan*, 100, 50-59.
- Lacaze, L., Le Gal, P., Le Dizès, S., 2005. Elliptical instability of the flow in a rotating shell. *Phys. Earth Planet. Int.*, Volume 151, pp. 194-205.
- Lacaze, L., Herreman, W., Le Bars, M., Le Dizès, S., Le Gal, P., 2006. Magnetic field induced by elliptical instability in a rotating spheroid. *Geophys. Astrophys. Fluid Dyn.* 100, 299–317.
- Le Bars, M., Le Dizès, S., 2006. Thermo-elliptical instability in a rotating cylindrical shell. *J. Fluid Mech.* 563, 189–198.
- Le Bars, M., Le Gal, P., 2007. Experimental analysis of the stratorotational instability in a cylindrical Couette flow. *Phys. Rev. Lett.* 99, 064502.
- Le Bars, M., Lacaze, M., Le Dizès, S., Le Gal, P., Rieutord, M., 2010. Tidal instability in stellar and planetary binary system. *Phys. Earth Planet. Int.*, 178 (1), p.48-55.
- Le Dizès, S., Laporte, F., 2002. Theoretical predictions for the elliptic instability in a two-vortex flow. *J. Fluid Mech.* 471, 169–201.
- Leweke, T., Williamson, C. H. K., 1998. Cooperative elliptic instability of a vortex pair. *J. Fluid Mech.* 360, 85–119.
- Lister, J. R., Buffett, B. A., 1998. Stratification of the outer core at the core-mantle boundary, *Phys. Earth Planet. Inter.*, 105, 5-19.
- Lubow, S. H., Pringle, J. E., Kerswell, R. R., 1993. Tidal instability of accretion disks. *Ap. J.* 419:758-67.
- Malkus, W. V. R., 1993. Energy sources for planetary dynamos. In *Lectures on Solar and Planetary Dynamos*, ed. MRE Proctor, AD Gilbert, pp. 161-79. Cambridge, UK: Cambridge Univ. Press.
- Meunier, P., Ehrenstein, U., Leweke, T., Rossi, M., 2002. A merging criterion for two-dimensional co-rotating vortices. *Phys. Fluids* 14, 2757–2766.
- Moore, D. W., Saffman, P. G., 1975. The instability of a straight vortex filament in a strain field. *Proc. R. Soc. Lond. A* 346, 413–425.
- Rieutord, M., 2003. Evolution of rotation in binaries: physical processes. *Stellar Rotation*, Proc. IAU Symp. 215, 394–403.
- Ryu, D., Goodman, J., 1994. Nonlinear evolution of tidally distorted accretion disks: Two-dimensional simulations. *Ap. J.* 422:269-88.
- Stanley, S., Mohammadi, A., 2008. Effects of an outer thin stably stratified layer on planetary dynamos. *Phys. Earth Planet. Int.* 168, 179-190.
- Sumita, I., Yoshida, S., 2002. Thermal interaction between the mantle, outer and inner cores, and the resulting structural evolution of the core. *Earth’s Core: Dynamics, Structure, Rotation*, Am. Geophys. Union, Washington, pp. 213-231.
- Tilgner, A., Busse, F. H., 1997. Finite-amplitude convection in rotating spherical fluid shells. *J. Fluid Mech.*, 332:359-376.
- Widnall, S. E., Bliss, D., Tsai, C.-Y., 1974. The instability of short waves on a vortex ring. *J. Fluid Mech.* 66, 35–47.
- Williams, G. E., 1994. Resonances of the fluid core for a tidally decelerating Earth: Cause of increased plume activity and tectonothermal reworking events? *Earth Planet. Sci. Lett.* 128, 155-167.

Table 1. List of relevant dimensionless parameters with the explored numerical ranges as well as their typical values in the Earth’s and Io’s cores.

Dimensionless parameters	Definition	Numerical ranges	Earth & Io’s core estimates
Eccentricity	$\varepsilon = \frac{b^2 - a^2}{a^2 + b^2}$	0 – 0.32	10^{-7} – 10^{-4}
Core radius ratio	η	0 – 0.3	0.35 – ?
Oblateness	c/b	0.86 – 1	997/100 – 995/100
Reynolds number	$Re = \Omega R_{eq}^2 / \nu$	$0 \leq 10^3$	10^{15} – 10^{13}
Ekman number	$E_k = 1/Re$	≥ 0.001	10^{-15} – 10^{-13}
Ekman number based on the gap	$E = ((1 - \eta)^2 Re)^{-1}$	≥ 0.002	10^{-15} – 10^{-13}
Prandtl number	$Pr = \nu / \kappa$	1	0.25 – 0.25
Rayleigh number	$Ra = \frac{\alpha g_0 (T_i - T_e) d^3}{\kappa \nu}$	$-3.8 \cdot 10^5$ – 10^6	10^{23} – ? ($< Ra_c$)
Flux-based Rayleigh number	$Ra_Q^* = Ra Nu E^3 / Pr^2$	$-2.6 \cdot 10^{-5}$ – 0.24	10^{-13} – ?
Nusselt number	$Nu = Q_{total} / Q_{conduction}$	1 – 5.6	10^6 – ?
Modified Nusselt number	$Nu^* = \frac{Nu E}{Pr}$	≥ 0.002	10^{-8} – ?
Rossby number	$Ro = \frac{\sqrt{\frac{1}{V} \int U^2 d\tau}}{\Omega R_{eq}^2}$	0 – 0.4	10^{-6} – ?

Figure 1. Schematic representation of the considered problem. The gravity field shown here in the equatorial plane is calculated explicitly, assuming that the outer boundary is an isopotential.

Figure 2. Evolution of the modified Nusselt number in the case of a rotating spherical shell ($\varepsilon = 0$) for $Pr = 1$, $\eta = 0.3$ and $Re = 344$. (a) Our computations are compared with a compilation of numerical and experimental results given by Aurnou (2007). (b) Our computations are compared with the scaling law (6) given by Christensen (2002).

Figure 3. (a) Influence of the Rayleigh number on the growth rate of the tidal instability for $\varepsilon = 0.317$, $c = \frac{a+b}{2}$, $Pr = 1$ and $Re = 344$ or $Re = 688$. The growth rate given by equation (7) is also shown, taking into account a classical damping by a surfacic viscous term $-K/\sqrt{E_k}$, where K is a constant of order 1 (Lacaze et al. 2005). The values of K have been determined by matching the theoretical value with the numerical one at $Ra = 0$, giving $K = 3.07$ for $Re = 344$ and $K = 2.91$ for $Re = 688$. (b) Evolution of the growth rate of the tidal instability with the Rossby number, calculated following the scaling law given by Christensen and Aubert (2006) $Ro = 0.85 (Ra_Q^*)^{0.41}$. For $Re = 344$, the instability disappears for $Ro \approx 0.25$.

Figure 4. Comparison between the convective flows in the absence of tidal instability (a, $\varepsilon = 0$) and in the presence of tidal instability (b, $\varepsilon = 0.317$) for the same values of the Reynolds number $Re = 344$, the Rayleigh number $Ra = 18762$ and the Prandtl number $Pr = 1$. The vertical velocity is shown in three different planes. Also shown in (b) is an iso-surface of the norm of the velocity $\|\mathbf{u}\| = 0.19$, which clearly exhibits the 'S' shape of the spin-over mode.

Figure 5. (a) Influence of the Reynolds number on the Nusselt number for a convective flow with $\varepsilon = 0.317$, $c = \frac{a+b}{2}$, $Pr = 1$ and $Ra = 18762$. (b) Evolution of the Nusselt number with the Rayleigh number in spherical and ellipsoidal ($\varepsilon = 0.317$, $c = \frac{a+b}{2}$) shells for $Pr = 1$ and $Re = 344$ or $Re = 688$. Note that the classical dependance of the critical Rayleigh for the convection $Ra_c \propto Re^{4/3}$ (see Tilgner and Busse (1997) for instance) can be observed: the decrease of the Reynolds number modifies the threshold and then, increases the convective motions.

Figure 6. Visualization of the reduced temperature T in the case of a stratified layer under a convective zone ($Re = 344$, $c = \frac{a+b}{2}$). The inner and outer boundaries verify $T = 0$ and at a ratio $\eta_2 = 0.7$, a temperature $T = 1$ is imposed such that the Rayleigh number based on the thickness of the shell is $Ra = 18762$, whereas the Rayleigh number based on η_2 is equal to $Ra_2 = Ra \frac{(1-\eta_2)^3}{(1-\eta)^3} \approx 1512$. (a) Temperature in the equatorial plane for a spherical shell of outer radius $R_{eq} = c$. (b) Temperature in the equatorial plane and surface of iso-value $\|\mathbf{u}\| = 0.19$ at saturation of the tidal instability for the corresponding ellipsoidal shell at $\varepsilon = 0.317$.

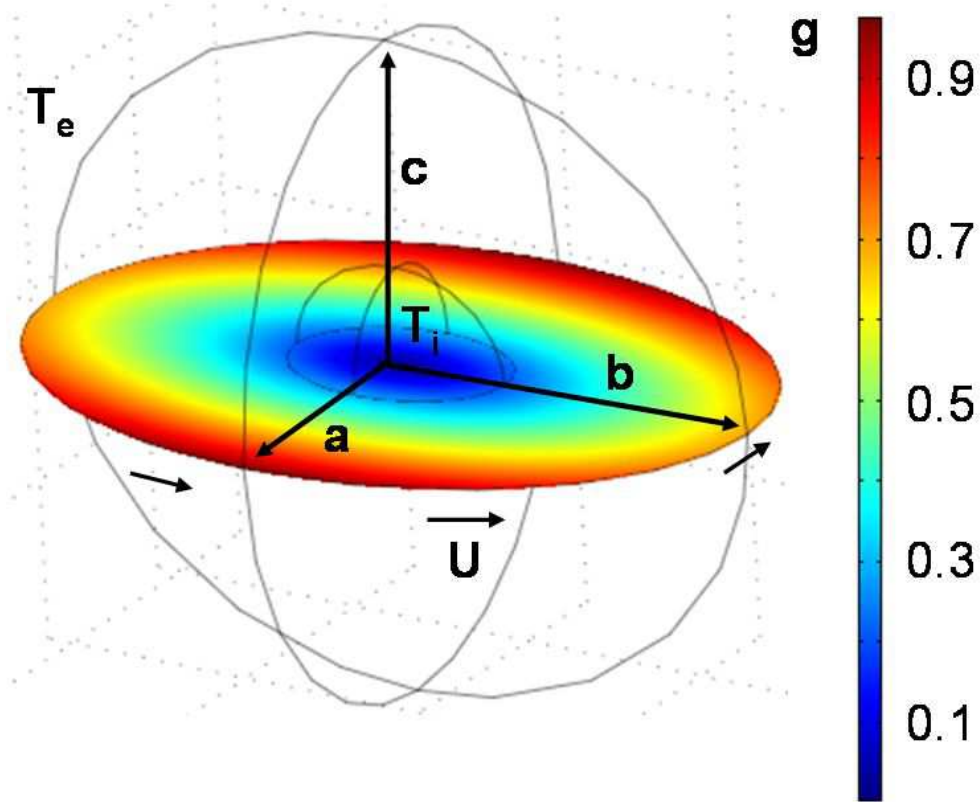


Figure 1.

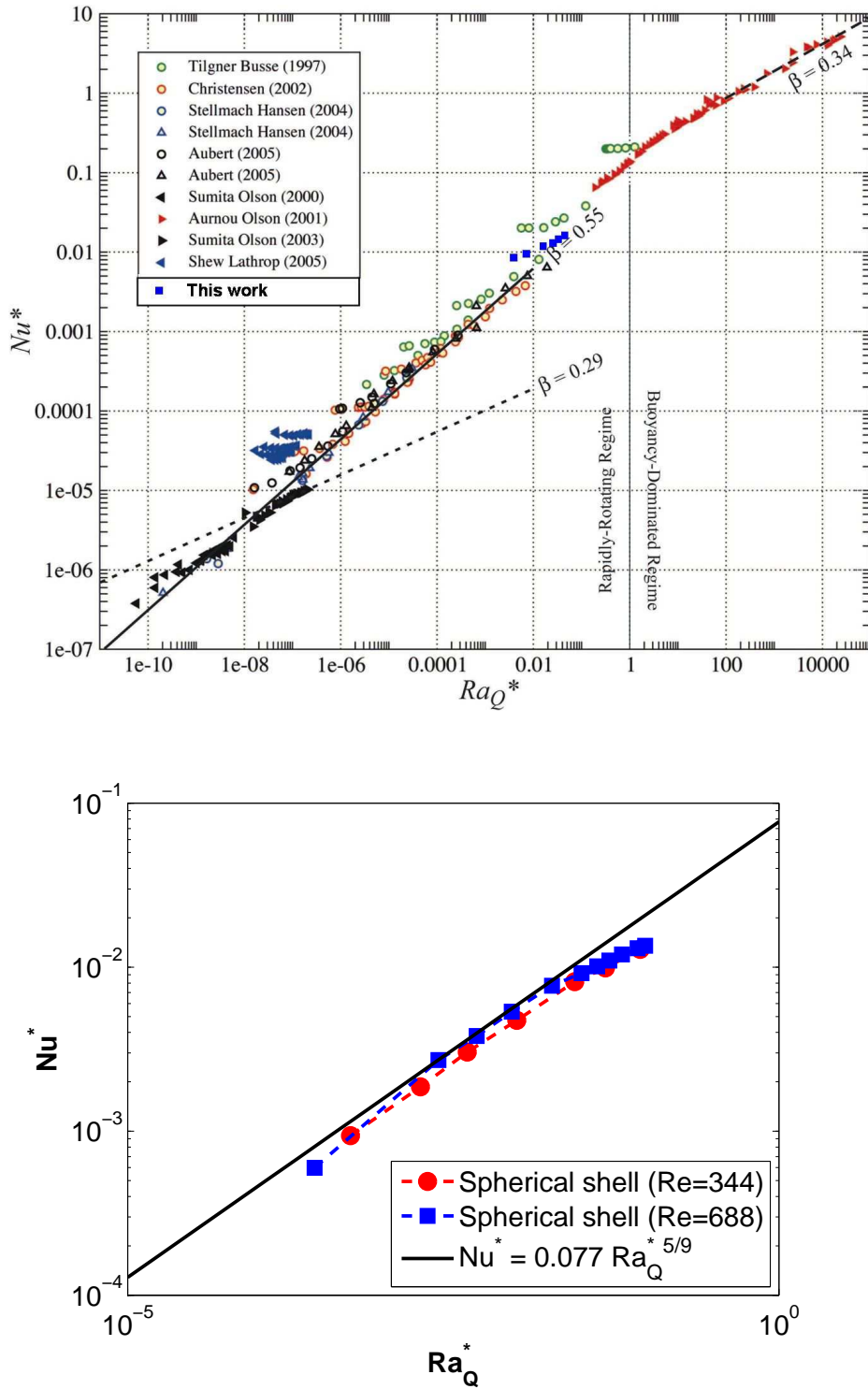


Figure 2. (a) Upper figure. (b) Lower figure.

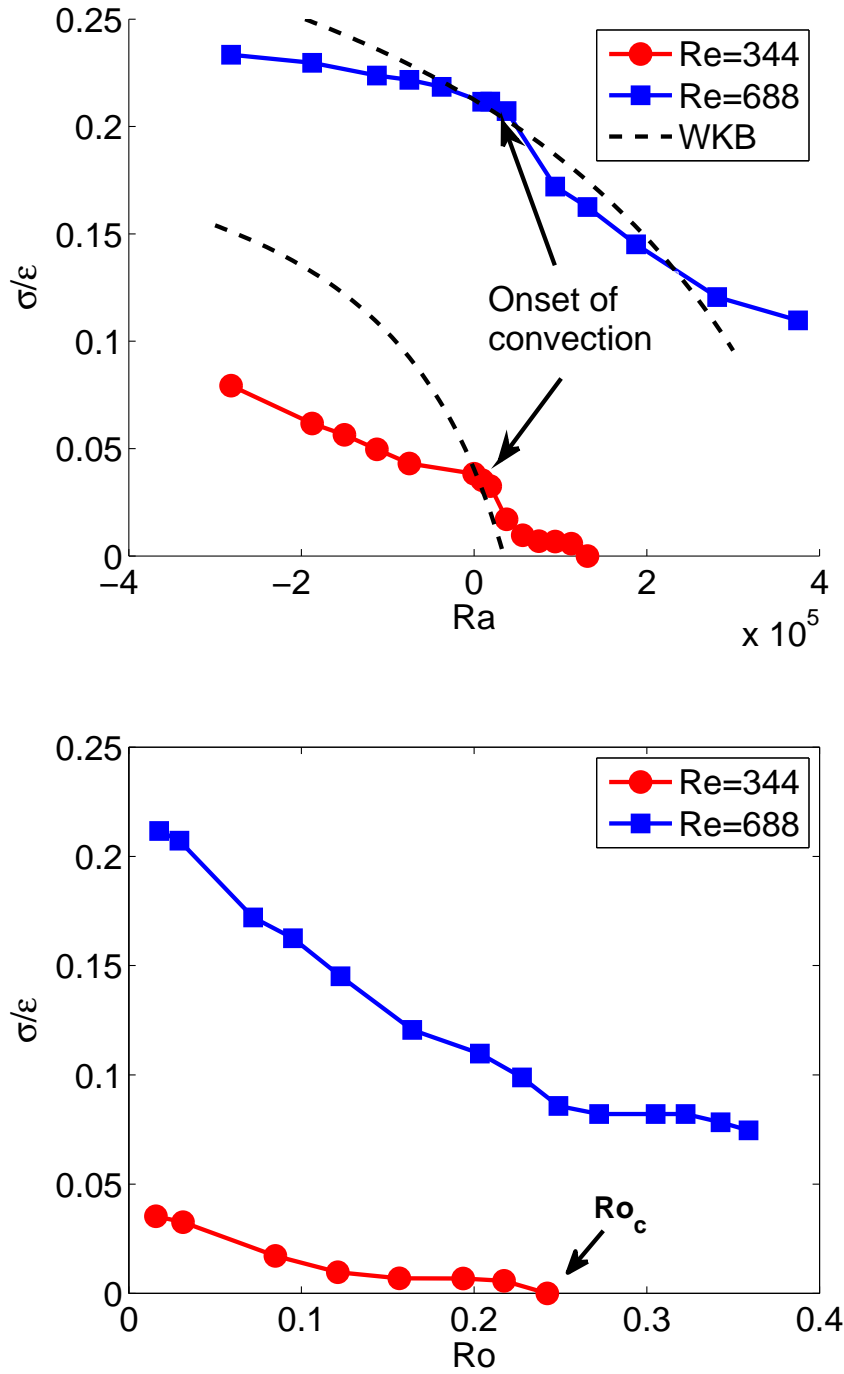


Figure 3. (a) Upper figure. (b) Lower figure.

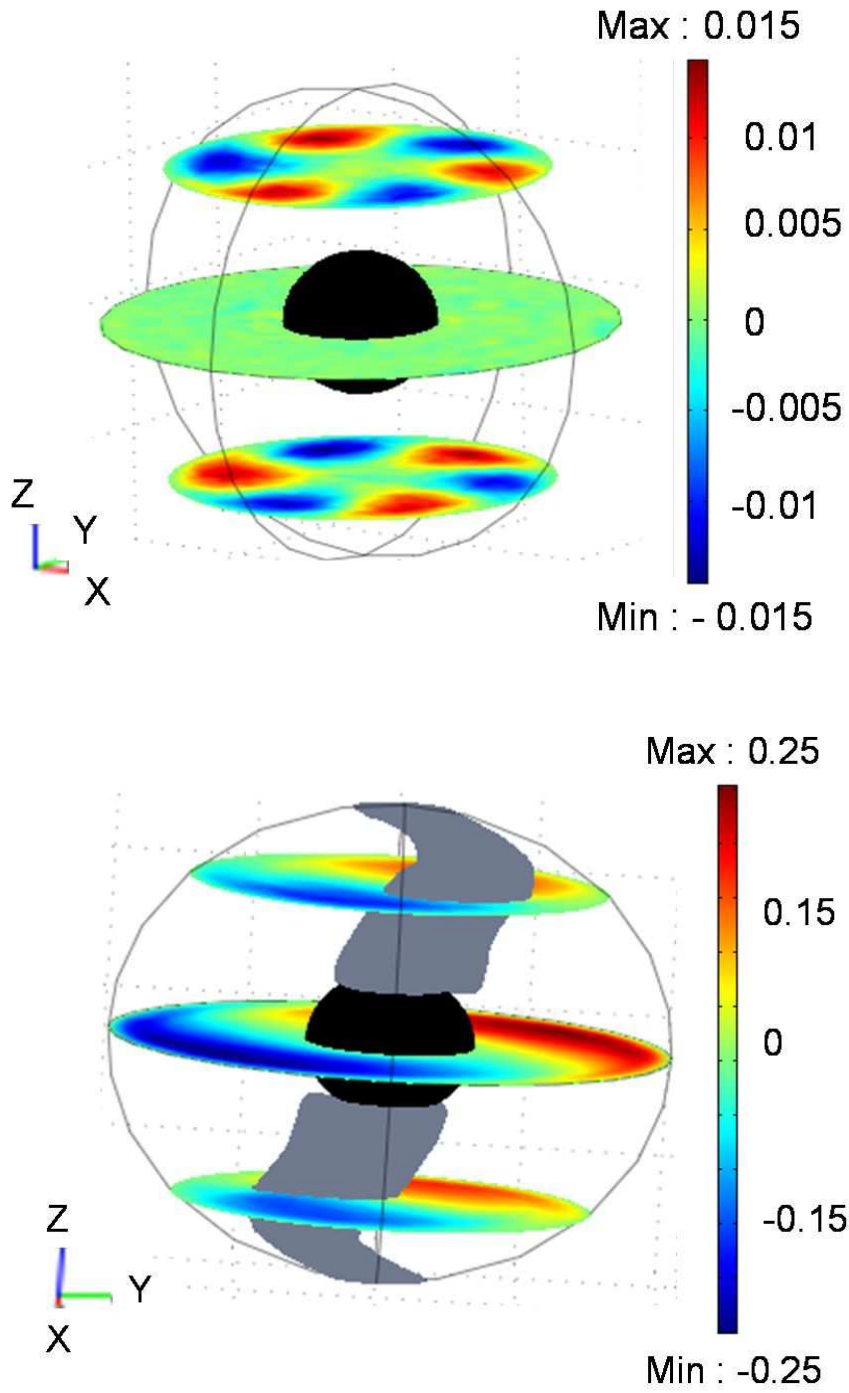


Figure 4. (a) Upper figure. (b) Lower figure.

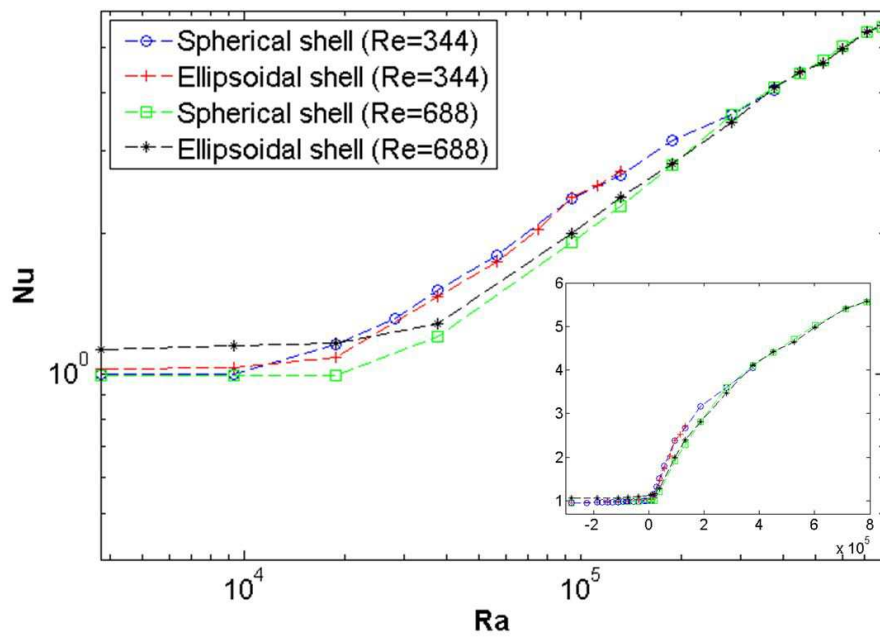
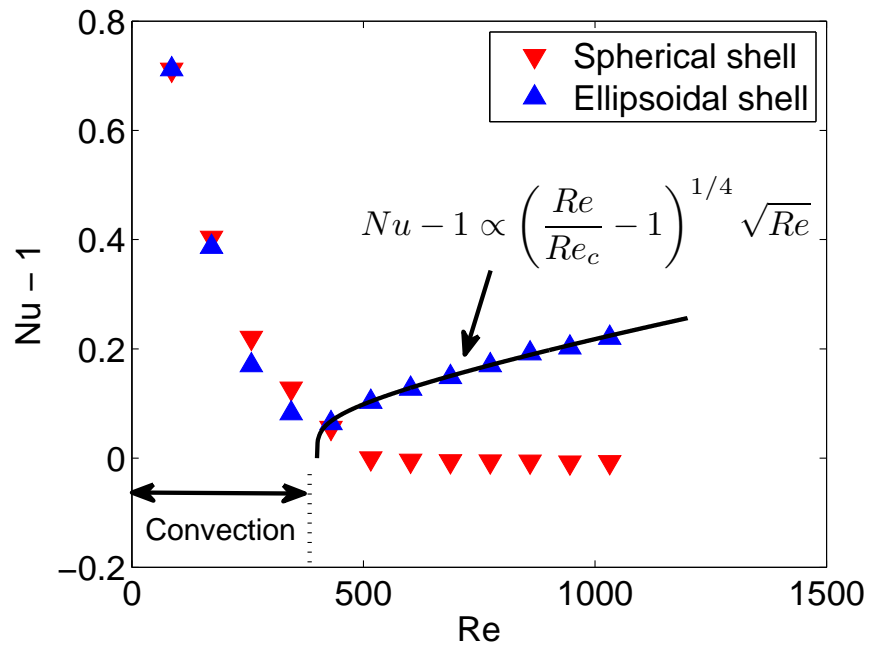


Figure 5. (a) Upper figure. (b) Lower figure.

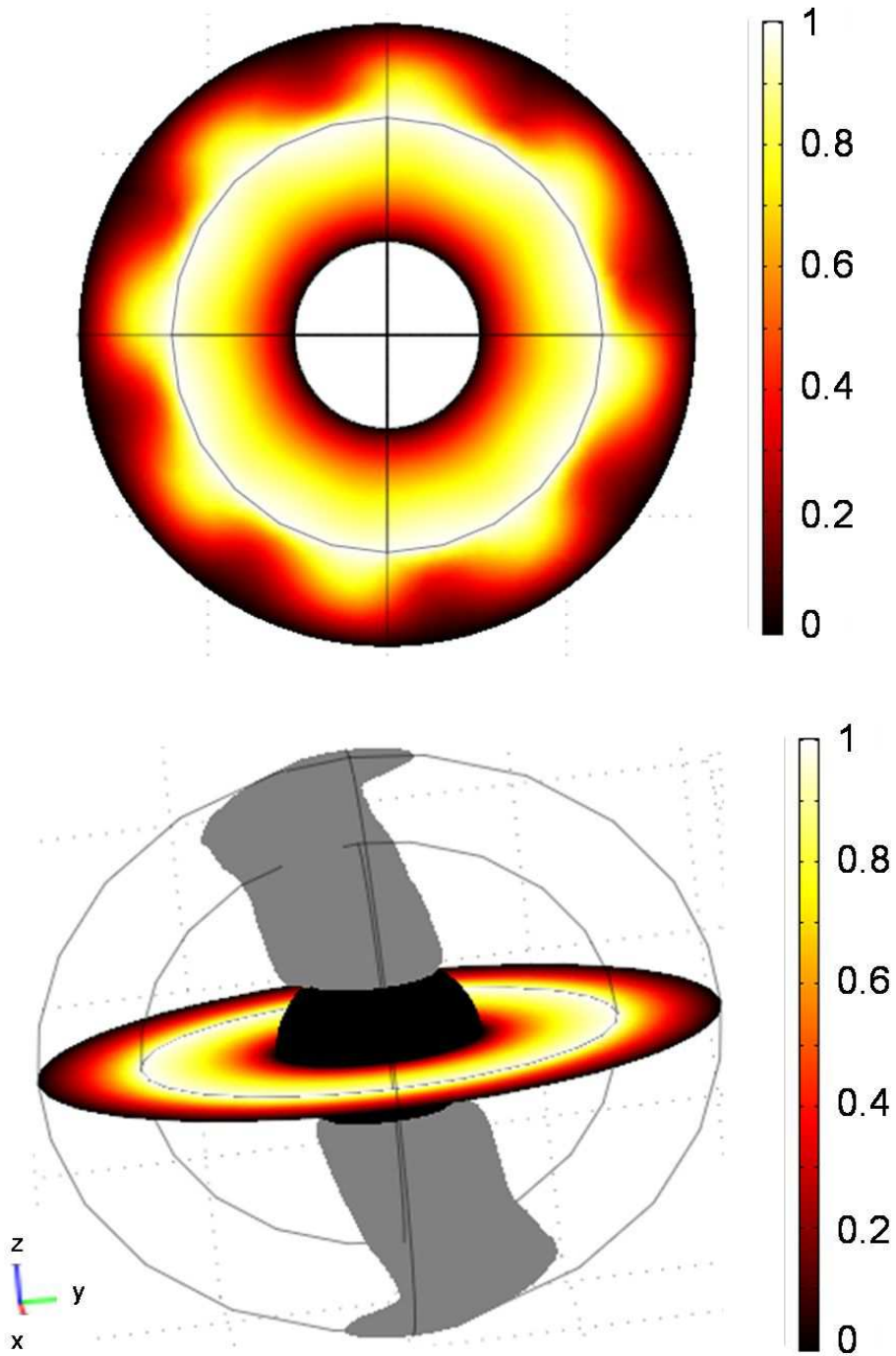


Figure 6. (a) Upper figure. (b) Lower figure.